A R C H I W U M I N S T Y T U T U I N Ż Y N I E R I I L Ą D O W E J
Nr 12 ARCHIVES OF INSTITUTE OF CIVIL ENGINEERING 2012

PRACTICAL ASPECTS OF STRAINS, STRESSES AND INTERNAL FORCES ESTIMATION DURING FIELD AND LABORATORY TESTS OF CORRUGATED CULVERTS

Leszek KORUSIEWICZ[*], Grzegorz CHRUŚCIELSKI[*], Robert JASIŃSKI[**]
[*]) PhD Mech. E., Wrocław University of Technology, Poland
[**]) MSc Mech. E., Wrocław University of Technology, Poland

Abstract

Full-size tests of steel and polymer culverts are of significant importance because results of such tests give an insight into the actual behavior of the structures under working conditions. The experimental evidence so gathered is a basis for putting forward computation models and their verification. For many years now one of the present authors has been involved in natural-scale laboratory and field tests of corrugated culverts. The submitted paper intends to present some practical aspects concerning the experiments carried out. Various gauges applied in the tests are described. Several useful formulas derived for calculating stresses and internal forces for various corrugation patterns of tested culverts are also included.

Key words: full-size tests, corrugated culverts, strains, stresses, internal forces

1. INTRODUCTION

The behaviour of in-ground conduits has been the subject of extensive study since the beginning of the 20th century. Buried structures such as sewers, pipes and tunnels have to be designed to support not only the dead loading of the soil providing cover but also a live loading at the ground surface. Many full-scale tests have been carried out in the field to validate long-term performance and load bearing capacity of these structures [1–9]. In contrast to that only few tests of life-size structures have been performed under fully controlled laboratory conditions [10–12]. Experimental data obtained under such conditions is urgently needed in order to verify numerical and analytical programs intended for computational analysis of that type of structures.

The first of the present authors has been long involved in practical investigations on buried flexible structures [13–18]. Of special importance are life-size laboratory tests conducted at the Road and Bridge Research Institute, Poland. To

our knowledge, no such tests have been performed so far elsewhere in Europe. The willingness to share the engineering experience gathered has been the chief motive behind the present publication.

2. MEASUREMENT INSTRUMENTATION

The quantities measured most often in investigating the structures in question are strains and displacements at a culvert shell and forces acting on it from the surrounding soil.

2.1Strains

Strains are measured with resistance strain gauges. The transducers are placed at the outer and inner side of the shell. In corrugated sheet culverts these are ridges of the form pattern wave (point G) and valleys (point D) – Fig. 1.

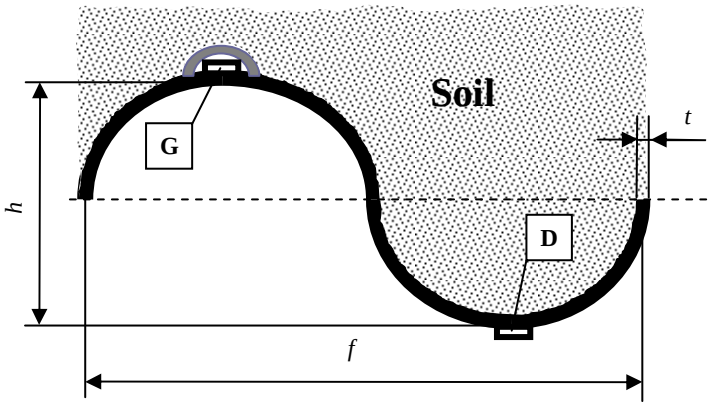

Figure 1. Geometry of sheet panel and strain pick-up location (points D and G)

In order to mount a strain gauge at the outer shell surface one has to expose an area of the sheet and leave it exposed throughout the measurement period. It has been found that pressure exerted by the soil on the gauge distorts the recorded values of strains due to internal forces in the shell. To overcome the problem some investigators choose to place the pick-ups solely at the inner side of the culvert – Fig. 2 – at the cost of losing the track of strains (stresses) at the cross-section outermost fibres. Complex loading conditions of the culvert shell result in a plane stress rather than unidirectional one at its free surface. In order to determine longitudinal and circumferential stresses one has to record strains along those two directions. As can be seen in Fig. 2, the bidirectional strain rosettes were attached at points G and D. Two commercial variations of such gauges are shown in Fig. 3, the one on the right having the advantage of measuring the two strains exactly at the same point.

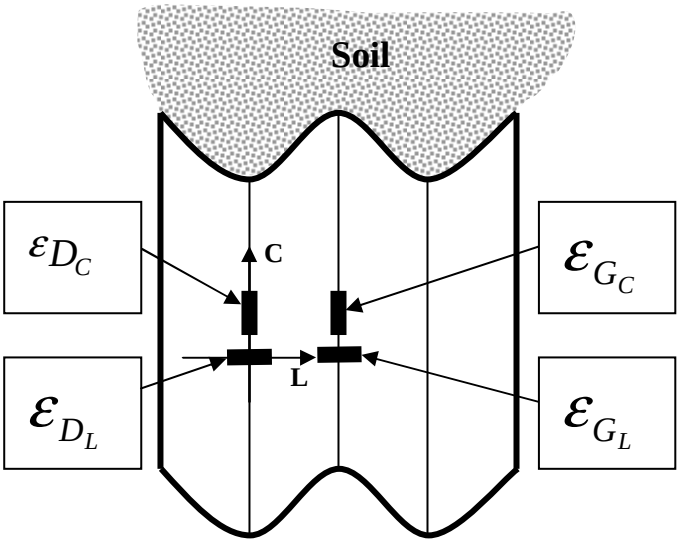

Figure 2. Strain gauge location at the inner side of the culvert panel

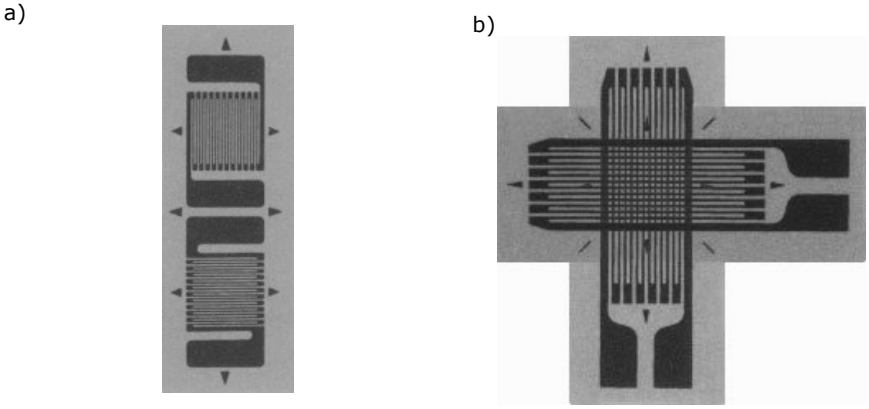

Figure 3. Bidirectional strain rosettes

2.2Deformations

Displacements are measured using a variety of pick-up devices. Those used most often include tachymeters, laser range finders, dial indicators and LVDTs – Fig. 4.

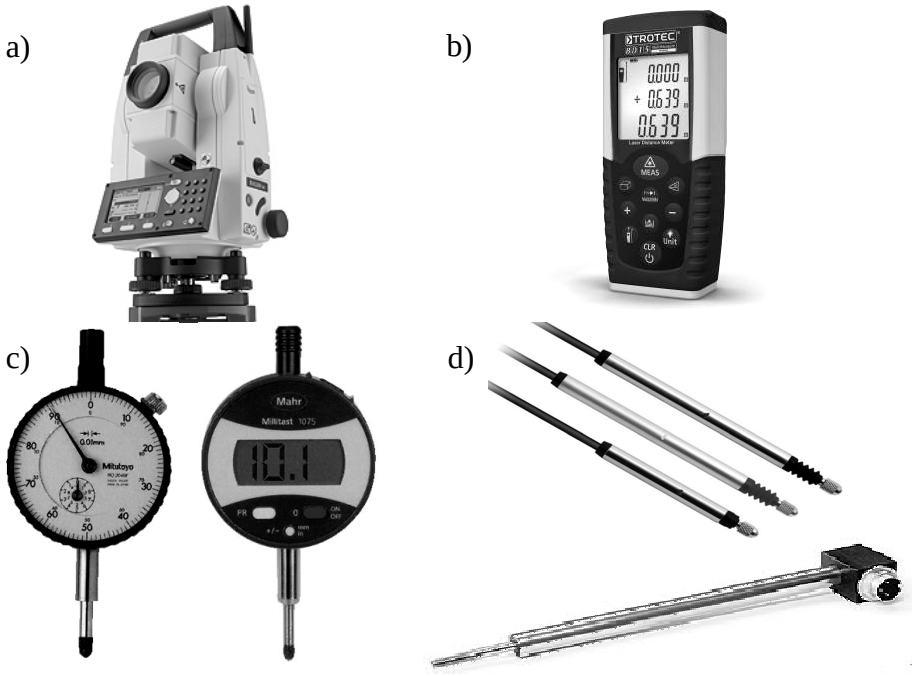

Figure 4. Displacement measuring devices: a – tachymeter, b – laser range finder, c – dial indicators, d – LVDTs

In field tests of large objectslaser range finders are the best choice. There is no need for mounting fixtures, as actually there is no mechanical contact between an object and the device since the three-dimensional positions of specific points on an object being determined first are the only prerequisite. This tachymeter's ability to determine all the three components of the displacement of a point is its most interesting feature. Dial indicators and inductive LVDTs are preferred in investigating smaller objects or in lab experiments in view of their greater accuracy. That advantage however loses much of its worth if the displacement does not act exactly along the axis of the device spindle.

Dial indicators and inductive LVDTs require mounting jigs that can be attached to the object tested or be stand-alone fixtures. In the first case changes in location of given points are measured with respect to the fixed reference data – Fig. 5a. In the second case – Fig. 5b – relative changes in position are detected. That mode of recording provides an investigator with a sufficient body of data if a change in vertical or horizontal diameter is everything that is required. It is to be noted that the vertical-to-horizontal diameter ratio is frequently used as a structural failure criterion.

a) b)

Figure 5. Various arrangements of inductive displacement pick-ups

The inductive displacement pick-ups are the only ones from among those listed earlier that enable an investigator to perform continuous recording of deformation in dynamic tests. The measuring set-up comprises auxiliary equipment for acquiring signals, processing and storing data – a typical workflow pattern in modern engineering practice.

2.3. Earth pressure

To measure total pressure in earth fills and pressures on the surface of tunnel linings etc. earth pressure cells are used – Fig. 6. The transducers have usually the form of circular or rectangular sandwich plates filled with oil. Signals from the internal pressure transducers are sent to the readout location. Installing the cells must follow strictly a manufacturer's recommended procedure since physical conditions of the surrounding medium (soil moisture, index of compaction) have a significant effect on the results of measurement.

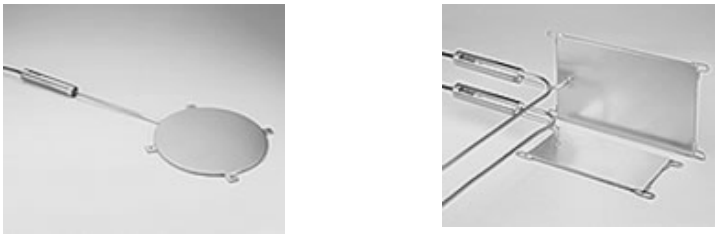

Figure 6. Earth pressure cells

If corrugated sheet lining is used, the cells should be placed at a distance of 2-5 cm from the lining perpendicular to the normal. An actual field arrangement of a pressure cell designed by Wrocław University of Technology can be seen in Fig. 7.

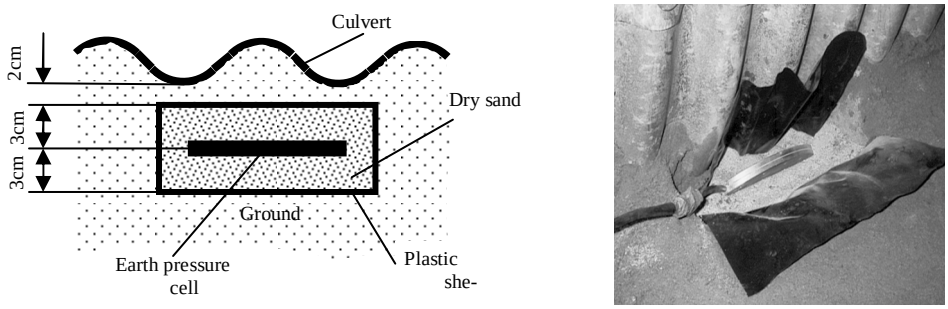

Figure 7. Earth pressure cell arrangement

3. DETERMINATION OF STRESSES

Stress components are calculated from strain components determined according to principles presented in Sect. 2.1. The Hooke's law as applied to plane stress conditions gives:

$$\varepsilon_x = \frac{1}{E}\left(\sigma_x - \nu\sigma_y\right),\ \ \varepsilon_y = \frac{1}{E}\left(\sigma_y - \nu\sigma_x\right),\ \ \varepsilon_z = -\frac{\nu}{E}\left(\sigma_x + \sigma_y\right),$$
$$\gamma_{xy} = \frac{1}{G}\tau_{xy} \tag{3.1}$$

Solving the first two equations with respect to σ_x and σ_y we get:

$$\sigma_x = \frac{E}{1-\nu^2}\left(\varepsilon_x + \nu\varepsilon_y\right),\ \ \sigma_y = \frac{E}{1-\nu^2}\left(\varepsilon_y + \nu\varepsilon_x\right) \tag{3.2}$$

With strains given at points D and G (Figs 1 & 2) the circumferential and longitudinal stresses will be:

$$\sigma_{D_C} = \frac{E}{1-\nu^2}\left(\varepsilon_{D_C} + \nu\varepsilon_{D_L}\right),\ \ \sigma_{D_L} = \frac{E}{1-\nu^2}\left(\varepsilon_{D_L} + \nu\varepsilon_{D_C}\right)$$
$$\sigma_{G_C} = \frac{E}{1-\nu^2}\left(\varepsilon_{G_C} + \nu\varepsilon_{G_L}\right),\ \ \sigma_{G_L} = \frac{E}{1-\nu^2}\left(\varepsilon_{G_L} + \nu\varepsilon_{G_C}\right) \tag{3.3}$$

where: σ_{D_C}, σ_{G_C}, ε_{D_C}, ε_{G_C} – circumferential stresses and strains at points D and G ; σ_{D_L}, σ_{G_L}, ε_{D_L}, ε_{G_L} – longitudinal stresses and strains at points D and G ; E – Young's modulus; ν – Poisson's ratio.

4. DETERMINATION OF INTERNAL FORCES

In longitudinal cross-sections of the shell (perpendicular to the circumferential direction) the usual set of internal forces arise: bending moments, normal forces, shearing forces. For the first two to be determined it is sufficient to have the σ_{D_C} and σ_{G_C} values. For the two different cross-sections shown in Fig. 8 the circumferential stress values at points D and G (as stress values at the outermost fibers, see Fig. 1) can be given as:

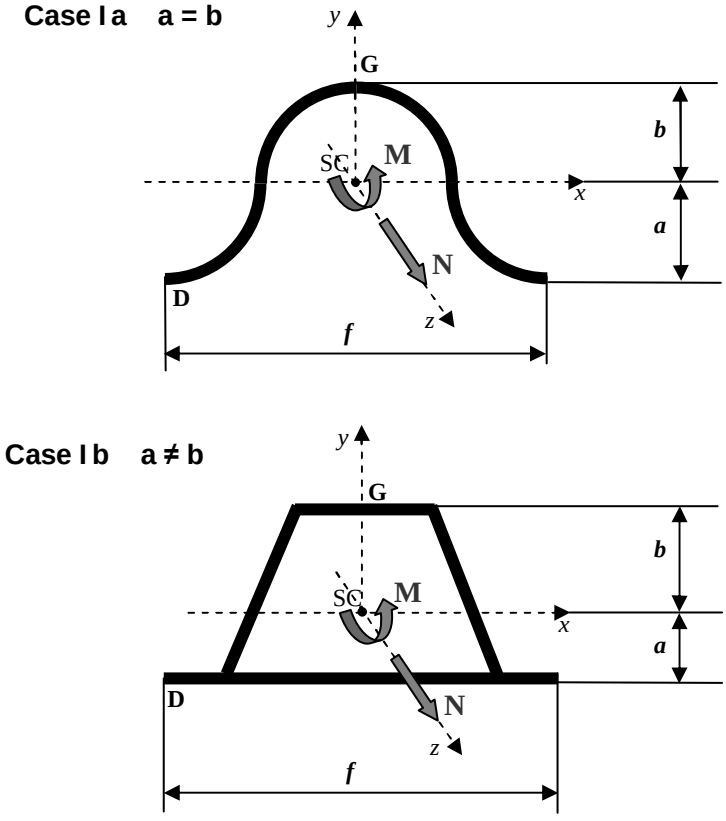

Figure 8. Cross-sectional normal forces and bending moments

$$\sigma_{D_C} = \frac{N}{A} + \frac{M}{I}a\,,\quad \sigma_{G_C} = \frac{N}{A} - \frac{M}{I}b \tag{4.1}$$

It follows then:

$$\sigma_{D_C} - \sigma_{G_C} = \frac{M}{I}(a+b) \tag{4.2}$$

Hence:

$$M = \frac{\sigma_{D_C} - \sigma_{G_C}}{a+b} I \tag{4.3}$$

Similarly:

$$b\sigma_{D_C} = \frac{b\,N}{A} + \frac{M}{I} ab\,, \quad a\sigma_{G_C} = \frac{a\,N}{A} - \frac{M}{I} ba \tag{4.4}$$

Hence:

$$b\sigma_{D_C} + a\sigma_{G_C} = \frac{N}{A}(a+b) \tag{4.5}$$

and finally

$$N = \frac{b\sigma_{D_C} + a\sigma_{G_C}}{a+b} A \tag{4.6}$$

In the above equations: N – normal force, M – bending moment about the neutral axis, A – cross-sectional area, I – second moment of area about the neutral axis x, a and b – perpendicular distances to the neutral axis x.

Case I a: $a = b$

$$M = \frac{\sigma_{D_C} - \sigma_{G_C}}{a+a} I = \frac{\sigma_{D_C} - \sigma_{G_C}}{2a} I = \left(\frac{\sigma_{D_C} - \sigma_{G_C}}{2} \right) \frac{I}{a} \tag{4.7}$$

$$N = \frac{a\sigma_{D_C} + a\sigma_{G_C}}{a+a} A = \frac{a\left(\sigma_{D_C} + \sigma_{G_C}\right)}{2a} A = \left(\frac{\sigma_{D_C} + \sigma_{G_C}}{2} \right) A \tag{4.8}$$

Case I b: $a \neq b$

$$M = \frac{\sigma_{D_C} - \sigma_{G_C}}{a+b} I = \left(\sigma_{D_C} - \sigma_{G_C}\right) \frac{I}{a+b} \tag{4.9}$$

$$N = \frac{b\sigma_{D_C} + a\sigma_{G_C}}{a+b} A = \left(b\sigma_{D_C} + a\sigma_{G_C}\right) \frac{A}{a+b} \tag{4.10}$$

For corrugated sheet as in Fig. 1 we get: $a = b = (h + t)/2$, where h – wave height, t – sheet thickness. Substituting in formulas (4.7) and (4.8) the following: $m = M/f$, $n = N/f$, $I_f = I/f$, $A_f = A/f$, where f – wave length, we get:

$$m = \left(\frac{\sigma_{D_C} - \sigma_{G_C}}{2} \right) \frac{2 I_f}{h + t} = \left(\sigma_{D_C} - \sigma_{G_C} \right) \frac{I_f}{h + t} \tag{4.11}$$

$$n = \left(\frac{\sigma_{D_C} + \sigma_{G_C}}{2} \right) A_f = \left(\sigma_{D_C} + \sigma_{G_C} \right) \frac{A_f}{2} \tag{4.12}$$

The characteristics I_f [mm^4/mm] and A_f [mm^2/mm] are provided in manufacturers' data sheets.

If the circumferential stress at point G has been determined on the inner side of the tube (Fig. 2), then bending moments and normal forces within material can be found directly from (4.7) and (4.8) or (4.11) and (4.12) by replacing σ_{G_C} with $\sigma^*_{G_C}$:

$$\sigma^*_{G_C} = \frac{\sigma_{G_C} - \sigma_{D_C}}{2a - t} 2a + \sigma_{D_C} = \frac{\sigma_{G_C} - \sigma_{D_C}}{h} \left(h + t \right) + \sigma_{D_C} \tag{4.13}$$

The stress $\sigma^*_{G_C}$ is a modification of the stress σ_{G_C} which takes into account the fact that strain gauges in location G are not fitted at the external surface of a culvert. The resulting equations are as follows:

$$M = \frac{\sigma_{D_C} - \sigma^*_{G_C}}{a + a} I = \frac{\sigma_{D_C} - \sigma^*_{G_C}}{2a} I = \left(\frac{\sigma_{D_C} - \sigma^*_{G_C}}{2} \right) \frac{I}{a} \tag{4.14}$$

$$N = \frac{a\sigma_{D_C} + a\sigma^*_{G_C}}{a + a} A = \frac{a\left(\sigma_{D_C} + \sigma^*_{G_C} \right)}{2a} A = \left(\frac{\sigma_{D_C} + \sigma^*_{G_C}}{2} \right) A \tag{4.15}$$

$$m = \left(\frac{\sigma_{D_C} - \sigma^*_{G_C}}{2} \right) \frac{2 I_f}{h + t} = \left(\sigma_{D_C} - \sigma^*_{G_C} \right) \frac{I_f}{h + t} \tag{4.16}$$

$$n = \left(\frac{\sigma_{D_C} + \sigma^*_{G_C}}{2} \right) A_f = \left(\sigma_{D_C} + \sigma^*_{G_C} \right) \frac{A_f}{2} \tag{4.17}$$

By using the σ_{G_C} value associated with a point on the internal sheet side – Fig. 2 – we get the following expressions for bending moments and normal forces:

$$M = \frac{\sigma_{D_C} - \sigma_{G_C}}{2a - t} I = \left(\sigma_{D_C} - \sigma_{G_C} \right) \frac{I}{2a - t} \tag{4.18}$$

$$N = \left[(a-t)\sigma_{D_C} + a\sigma_{G_C}\right]\frac{A}{2a-t} \tag{4.19}$$

$$m = \left(\sigma_{D_C} - \sigma_{G_C}\right)\frac{I_f}{h} \tag{4.20}$$

$$n = \left[(h-t)\sigma_{D_C} + (h+t)\sigma_{G_C}\right]\frac{A_f}{2h} \tag{4.21}$$

5. CHARACTERISTICS OF CORRUGATED PANELS

Corrugated sheet is characterized by its bending stiffness *K* and membrane stiffness *D*. Assuming the nomenclature from Fig. 9 we get the following indexes of bending stiffness [19]:

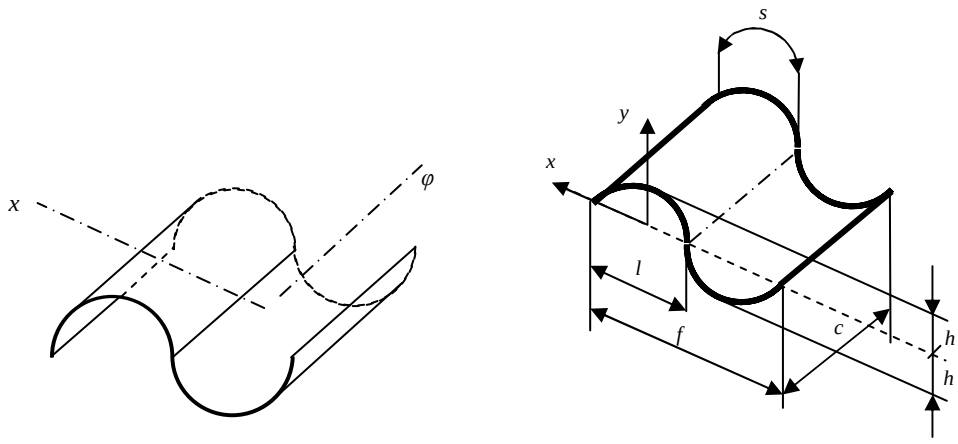

Figure 9. Geometry of sinusoid-shaped sheet.

$$K_\varphi = \frac{E\,I\,t}{l}; \quad K_x = \frac{E\,t^3}{12\left(1-\nu^2\right)}\frac{l}{s}; \quad K_{x\varphi} = \frac{E\,t^3}{12\left(1+\nu\right)}\frac{s}{l}. \tag{5.1}$$

Similarly, membrane stiffness is given by:

$$D_\varphi = E\,t\frac{s}{l}; \quad D_x = \frac{E\,t^3}{12\left(1-\nu^2\right)}\frac{l}{I}; \quad D_{x\varphi} = \frac{E\,t}{2\left(1+\nu\right)}\frac{l}{s}; \tag{5.2}$$

where: t – sheet thickness, E –Young's modulus, v – Poisson's ratio; and parameters s and I may be expressed as:

$$s = \int_{-l/2}^{l/2} \sqrt{1 + \left(\frac{dy}{dx}\right)^2}\, dx \tag{5.3}$$

$$I = \int_{x=-l/2}^{x=l/2} y^2 ds = \int_{-l/2}^{l/2} y^2 \sqrt{1 + \left(\frac{dy}{dx}\right)^2}\, dx \tag{5.4}$$

5.1. Determination of parameters *s* and *I* for a sinusoid arc

Assuming again the nomenclature from Fig. 9:

$$k = \frac{\pi h}{l}; \quad \delta = \sqrt{1 + \frac{1}{k^2}}; \quad \alpha = \arcsin(1/\delta) \tag{5.5}$$

and

$$A = \frac{2k\delta}{\pi} E(\alpha); \quad B = \frac{2}{3\pi}\left[K(\alpha) + \left(k^2 - 1\right)E(\alpha)\right]; \tag{5.6}$$

where: $K(\alpha)$, $E(\alpha)$ – the complete elliptic integrals of the first kind

$$K(\alpha) = \int_0^{\pi/2} \frac{d\phi}{\sqrt{1 - (\sin\alpha \sin\phi)^2}}; \quad E(\alpha) = \int_0^{\pi/2} \sqrt{1 - (\sin\alpha \sin\phi)^2}\, d\phi \tag{5.7}$$

;

parameters s and I may be expressed as:

$$s = Al; \quad I = Blh^2. \tag{5.8}$$

5.2. Determination of parameters *s* and *I* for a circle arc

Assuming now the nomenclature from Fig. 10:

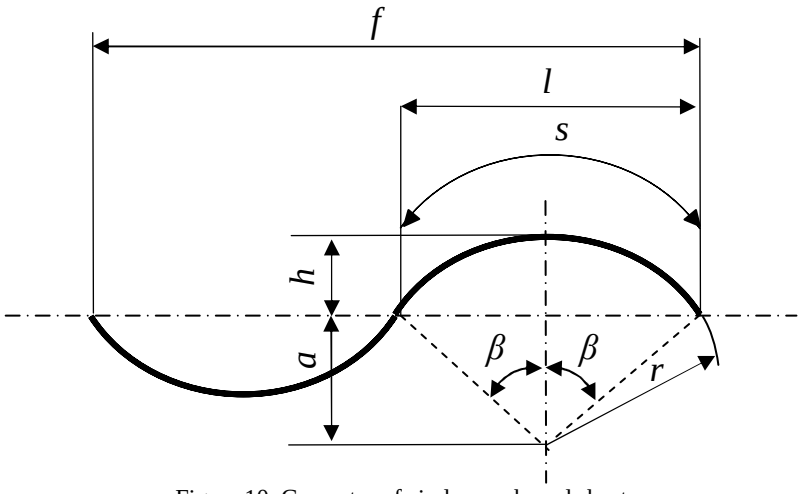

Figure 10. Geometry of circle arc-shaped sheet

$$\varphi = \frac{2h}{l}; \quad \beta = \arctan\varphi; \quad \rho = \frac{r}{h} = \frac{1}{\varphi \sin\beta}; \quad \alpha = \frac{a}{h} = \rho - 1; \tag{5.9}$$

and

$$A = \rho\beta\varphi; \quad B = \frac{1}{2}\left[A\left(\rho^2 + 2\alpha^2\right) - 3\rho\alpha\right]; \tag{5.10}$$

parameters *s* and *I* may be expressed as:

$$s = 2\beta r = Al; \quad I = \beta r\left(r^2 + 2a^2\right) - \frac{3}{2} r a l = B l h^2 . \tag{5.11}$$

5.3. Determination of internal forces using stiffness indexes K_φ and D_φ

Stiffness indexes K_φ and D_φ for the corrugated panel may be expressed as:

$$K_\varphi = E I_f; \quad D_\varphi = E A_f . \tag{5.12}$$

Internal forces *m* and *n* as given by (4.11) and (4.12) can be then rewritten as:

$$m = \left(\sigma_{D_C} - \sigma_{G_C}\right)\frac{K_\varphi}{E(h+t)}; \quad n = \left(\sigma_{D_C} + \sigma_{G_C}\right)\frac{D_\varphi}{2E}, \tag{5.13}$$

and those given by (4.20) and (4.21) — as:

$$m = \left(\sigma_{D_C} - \sigma_{G_C}\right)\frac{K_\varphi}{E\,h}; \quad n = \left[(h-t)\sigma_{D_C} + (h+t)\sigma_{G_C}\right]\frac{D_\varphi}{2\,E\,h}. \tag{5.14}$$

Stresses at the outermost fibers of the shell are:

$$\sigma_{D_C} = \frac{n}{D_\varphi}E + \frac{m}{K_\varphi}E\left(\frac{h+t}{2}\right); \quad \sigma_{G_C} = \frac{n}{D_\varphi}E - \frac{m}{K_\varphi}E\left(\frac{h+t}{2}\right), \tag{5.15}$$

while the extreme stresses on the inner shell side are:

$$\sigma_{D_C} = \frac{n}{D_\varphi}E + \frac{m}{K_\varphi}E\left(\frac{h+t}{2}\right); \quad \sigma_{G_C} = \frac{n}{D_\varphi}E - \frac{m}{K_\varphi}E\left(\frac{h-t}{2}\right). \tag{5.16}$$

6. FAILURE CRITERION

A failure criterion for (ductile) culvert material can be stated as follows: stress value at any point of a cross-section must be lower than the yield stress R_E of the culvert material.

The extreme normal stress values are the sum of σ_n due to normal force and σ_m due to bending moment. The two stresses are equal to:

$$\sigma_n = \left(\frac{\sigma_{D_C} + \sigma_{G_C}}{2}\right); \quad \sigma_m = \pm\left(\frac{\sigma_{D_C} - \sigma_{G_C}}{2}\right) \tag{6.1}$$

for σ_{D_C} and σ_{G_C} determined at both sides of the sheet (the outermost fibers), or

$$\sigma_n = \left(\frac{\sigma_{D_C} + \sigma^*_{G_C}}{2}\right); \quad \sigma_m = \pm\left(\frac{\sigma_{D_C} - \sigma^*_{G_C}}{2}\right) \tag{6.2}$$

for σ_{D_C} and σ_{G_C} determined at the inner side of the sheet.

It easily noted that the extreme stress values occur at the outermost fibers and therefore the failure criterion here takes the form:

$$\max\left(|\sigma_n| + |\sigma_m|\right) < R_E\,. \tag{6.3}$$

It is a simplified approach since the actual plane stress would require an equivalent stress value to be determined from the Mises–Huber criterion and then checked against the yield stress

$$\max(\sigma_{eq}) < R_E \tag{6.4}$$

REFERENCES

1. Selig E.T., Lockhart C.W., Lautensleger R.W.: *Measured performance of Newton Creek culvert*, Journal of the Geotechnical Engineering Division, Proceedings of ASCE, Vol. 105, No. GT9, 1979, pp. 1067-1087.
2. Kay J.N. et al.: *Instrumentation of a corrugated steel-soil arch overpass at Leigh Creek, South Australia*, ARRB Proceedings, Vol. 10, Part 3, 1980, pp. 57-70.
3. Byrne P.M. et al.: *Field measurements and analysis of a large-diameter flexible culvert*, Can. Geotech. J., Vol. 30. 1993, pp. 135-145.
4. Vaslestad J.: *Long-term behaviour of flexible large-span culverts*, Publica-tion No.74, Norwegian Pub. Roads Administration, Oslo 1994, pp. 38-56.
5. Kjartanson B.H. et al.: *Full-scale field tests on longitudinal uplift response of corrugated metal pipe*, Transportation Research Record 1656, Journal of TRB, 1999, pp. 80-87.
6. Vaslestad J., Madaj A., Janusz L.: *Field measurements of long-span corru-gated steel culvert replacing corroded concrete bridge*, Transportation Research Record 1814, Journal of TRB, 2002, pp 164-170.
7. Bęben D., Mańko Z.: *Analysis of shell in soil-steel bridges during backfill-ing*, Proc. of the Third International Conference on SEMC, Cape Town, South Africa 2007, pp. 822-827.
8. Flener E.B., Sundquist H.: *Field testing of a long-span arch corru- gated-steel culvert under dynamic and static loads*, Archives of Institute of Civil Engineering, No 1, 2007, Poznań Univer. of Technology, pp. 25-33.
9. Flener E.B., Sundquist H.: *Full-scale testing of two corrugated steel box culverts with different crown stiffness*, Archives of Institute of Civil Engineering, No 1, 2007, Poznań University of Technology, pp. 35-44.
10. Shmulevich I., Galili N.: *Deflections and bending moments in buried pipe*, Journal of Transportation Engineering, ASCE, Vol. 112, No. 4, 1986, pp. 345-357.
11. McVay M., Papadopoulos P.: *Long-term behaviour of buried large-span culverts*, Journal of Geotechnical Engineering, ASCE, Vol. 112, No. 4, 1986, pp. 424-442.
12. Brachman R.W.I, Moore I.D., Mak A.C.: *Ultimate limit state of deep-corrugated large-span box culvert*, Transportation Research Record 2201, Journal of TRB, 2010, pp 55-61.
13. Veslestad J., Korusiewicz L., Wysokowski A.: *General description of static and dynamic testing of instrumented steel culvert*, V International Conference - Durable and Safe Road Pavements, Kielce, 11-12 May 1999, pp. 215-221
14. Korusiewicz L.,Kunecki B.: *On boundary conditions in experimental and numerical models of steel culverts*, Proceedings Of The 8th SSTA Conference, Jurata, Poland, 12-14 October 2005; Shell Structures: Theory and Applications, pp. 573-576

15. Kunecki B., Korusiewicz L.: *Laboratory test of a full-scale soil-steel box-type culvert under road loads*, New horizons and better practices, Proceedings of the ASCE Structures Congress, Long Beach, California, 16-19 May 2007.
16. Korusiewicz L., Kunecki B.: *Influence of first loading cycles on a steel culvert behaviour*, 7th Youth Symposium on Experimental Solid Mechanics, 14-17 May 2008, Wojcieszyce, Poland.
17. Korusiewicz L., Kunecki B.: *Laboratory fatigue test of a full-scale steel culvert*, Proceedings of LCF6, Berlin, Germany, 8-12 September 2008, pp. 637-642.
18. Korusiewicz L., Kunecki B.: *Behaviour of the steel box-type culvert during backfilling*, Archives of Civil and Mechanical Engineering, Vol. XI, No. 3, 2011, pp. 637-650.
19. Girkmann K.: *Dźwigary powierzchniowe* [in Polish], Arkady, 1957, pp. 343-344.

Streszczenie

Testy przepustów stalowo-polimerowych naturalnej wielkości mają duże znaczenie, ponieważ ich rezultaty pozwalają poznać rzeczywiste zachowanie tych konstrukcji w warunkach użytkowania. Dowody eksperymentalne zebrane w ten sposób stanowią podstawę proponowania modeli obliczeniowych i ich weryfikacji. Od wielu lat jeden z autorów tej pracy jest zaangażowany w testy terenowe i laboratoryjne przepustów z blachy falistej naturalnych rozmiarów. Przedstawiona praca ma na celu przedstawienie pewnych praktycznych aspektów dotyczących opisanych eksperymentów. Opisano różne przyrządy pomiarowe stosowane w testach. Dołączono również pewne przydatne wzory do obliczania naprężeń i sił wewnętrznych (napięć) dla różnych wzorów fal badanych przepustów.

Słowa kluczowe: testy konstrukcji naturalnych rozmiarów, przepusty z blachy falistej, naprężenia, odkształcenia, napięcia